

Versatile Behavior of $[\text{Pt}_2\text{Ag}_4(\text{C}\equiv\text{C}-t\text{-Bu})_8]$: Synthesis, Structures, and Properties of $[\{\text{Pt}_2\text{Ag}_4(\text{C}\equiv\text{C}-t\text{-Bu})_8\}\{\text{Ag}(\text{bipy})\}]^{4+}$ and an Unprecedented Chain Polymeric Cocrystallization Adduct with a 2,2'-bipy Ligand

Irene Ara,[†] Juan Forniés,^{*,†} Julio Gómez,[‡] Elena Lalinde,^{*,‡} and M. Teresa Moreno[‡]

Departamento de Química Inorgánica, Instituto de Ciencia de Materiales de Aragón, Universidad de Zaragoza-Consejo Superior de Investigaciones Científicas, 50009 Zaragoza, Spain, and Departamento de Química-Grupo de Síntesis Química de La Rioja, UA-CSIC Universidad de La Rioja, 26001 Logroño, Spain

Received February 17, 2000

An unusual adduct, $[\{\text{Pt}_2\text{Ag}_4(\text{C}\equiv\text{C}-t\text{-Bu})_8(\text{bipy})\}]_\infty$ (**3**), has been obtained from the reaction of the hexanuclear cluster $[\text{Pt}_2\text{Ag}_4(\text{C}\equiv\text{C}-t\text{-Bu})_8]$ (**1**) with 2,2'-bipy independently of the molar ratio (1:1 or 1:excess) employed. The crystal structure of **3** shows the presence of an extended polymeric chain constructed by long-range, secondary misdirected $\text{Ag}\cdots\text{N}$ interactions between the cluster units and the 2,2'-bipy ligand. **3** is highly emissive in the solid state and in frozen solution. A considerable enhancement of the luminescence and a notable red shift in the emission maximum of **3** (λ_{max} 513 nm) relative to $[\text{Pt}_2\text{Ag}_4(\text{C}\equiv\text{C}-t\text{-Bu})_8]$ (**1**) (λ_{max} 476 nm) is observed. In an attempt to obtain an analogous polymeric chain based on higher nuclearity building blocks, the reaction between $[\{\text{Pt}_2\text{Ag}_8(\text{C}\equiv\text{C}-t\text{-Bu})_8\}(\text{OClO}_3)_2(\text{OCMe}_2)_2](\text{O}_2\text{-ClO}_2)_2]_\infty$ (**2**) and 2,2'-bipy was also examined. Treatment of **2** with 2,2'-bipy (molar ratio 1:4, Ag:bipy 1:0.5), however, produces $[\{\text{Pt}_2\text{Ag}_4(\text{C}\equiv\text{C}-t\text{-Bu})_8\}\{\text{Ag}(\text{bipy})\}_4](\text{ClO}_4)_4$ (**4**), in which the cluster unit acts as an octadentate bridging ligand toward four Ag(bipy) fragments. The use of a higher proportion of 2,2'-bipy (1:6 or 1:8 molar ratio) produces $[\text{Pt}_2\text{Ag}_8(\text{C}\equiv\text{C}-t\text{-Bu})_8(\text{bipy})_6](\text{ClO}_4)_4$ (**5**).

Introduction

Currently there is much interest in the preparation of polymeric materials containing metals mainly due to their potential practical applications and also because of the desire to understand the processes that govern their formation.¹ Much work has focused on coordination polymers, in particular metallopolymers containing Ag(I) or Cu(I), sustained by strong coordinated covalent bonds formed, in general, with *exo*-bidentate NN'-bridging donor ligands.² Weak noncovalent bonding interactions such as hydrogen bonds and $\text{M}\cdots\text{M}$, $\pi\cdots\pi$, or $\pi\cdots\text{M}$ stacking interactions have also been exploited to form multidimensional arrays.³ However, despite their interesting properties and chemistry, the design of polymer extended networks built upon preorganized polynuclear or cluster units is not developed so extensively.^{1c,4} Alkynyl groups are good σ -donor ligands, and considerable efforts have also been centered on the use of diynyl and functionalized alkynyl ligands to form polymetallic materials.^{1b,c,5} It has been shown that these ligands exhibit also very good π (η^2) coordinating capability, but only a few crystallographic examples of

polymeric derivatives involving alkynyl ligands have been reported.⁶ As a part of our work on the chemistry and properties of alkynyl–platinum-containing polynuclear complexes, we are interested in the exploration of σ -alkynyl platinate compounds as potential precursors for the construction of polymeric materials by using π -metal alkynyl bonds and perhaps also $\text{Pt}\cdots\text{M}$ bonding interactions.⁷ On the basis of cation– π and/or $\text{Pt}\cdots\text{M}$ interactions, we have succeeded in the construction of a new chain polymeric complex formed by

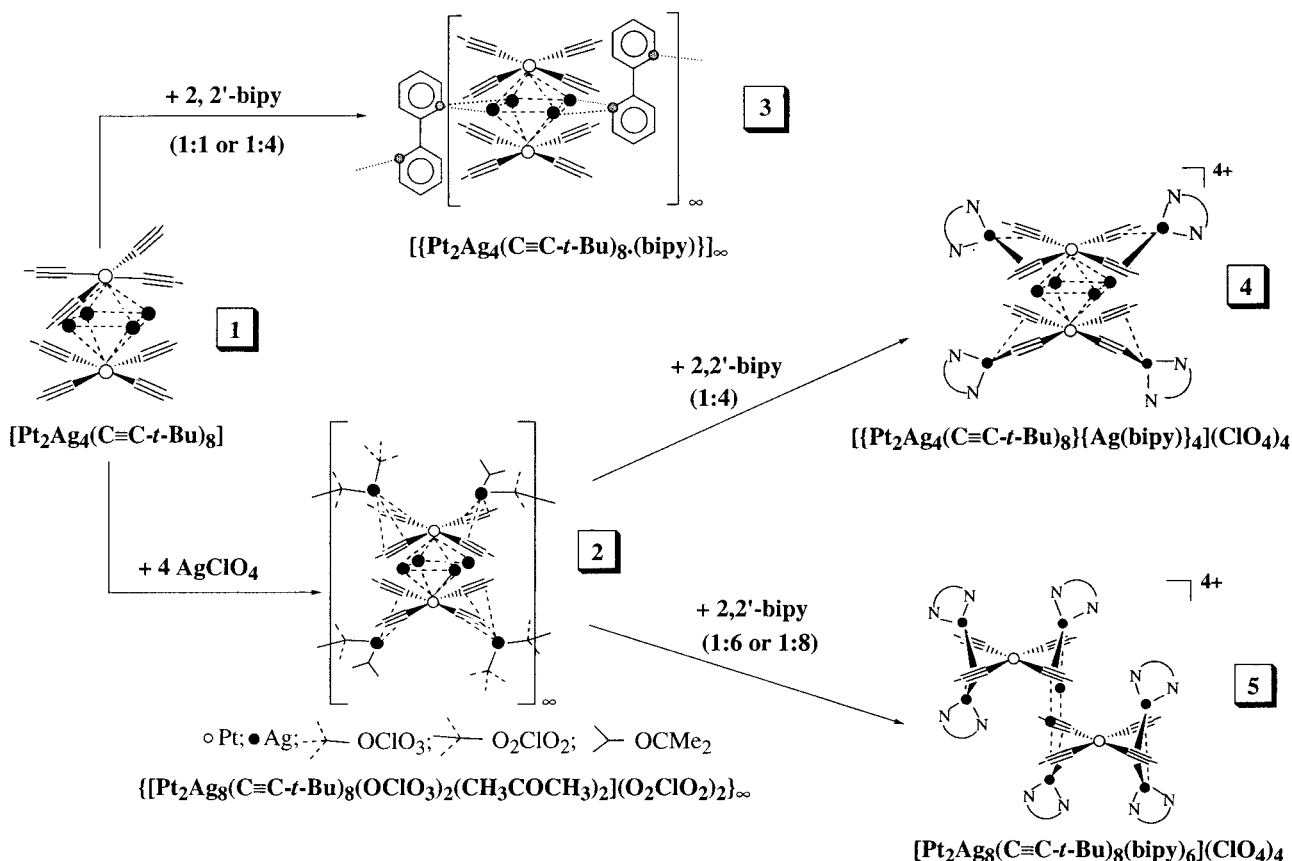
(2) (a) Robson, R.; Abrahams, S. F.; Batten, S. R.; Gable, R. W.; Hoskins, B. F.; Liu, J. In *Supramolecular Architecture*; Bein, T., Ed.; American Chemical Society: Washington DC, 1992; Chapter 19. For some recent works: (b) Janiak, C.; Uehlin, L.; Wu, H. P.; Klüfers, P.; Piotrowski, H.; Scharmann, T. G. *J. Chem. Soc., Dalton Trans.* **1999**, 3121. (c) McMorran, D. A.; Steel, P. *J. Inorg. Chem. Commun.* **1999**, 2, 368. (d) Wu, H. P.; Janiak, C.; Rheinwald, G.; Lang, H. *J. Chem. Soc., Dalton Trans.* **1999**, 183. (e) Suenaga, Y.; Yan, S. G.; Wu, L. P.; Kuroda-Sowa, T.; Maekawa, M.; Munakata, M. *J. Chem. Soc., Dalton Trans.* **1998**, 1121. (f) Fortin, D.; Drouin, M.; Turcotte, M.; Harveiy, P. D. *J. Am. Chem. Soc.* **1997**, 119, 531. (g) Withersby, M. A.; Blake, A. J.; Champness, N. R.; Hubberstey, P.; Li, W. S.; Schröder, M. *Angew. Chem., Int. Ed. Engl.* **1997**, 36, 2327. (h) Hannon, M. J.; Painting, C. L.; Errington, W. *Chem. Commun.* **1997**, 1805. (i) Blake, A. J.; Champness, N. R.; Khlobystov, A. N.; Lemenovskii, D. A.; Li, W. S.; Schröder, M. *Chem. Commun.* **1997**, 1339. (j) Carlucci, L.; Ciani, G.; Gudenberg, D. W. V.; Proserpio, D. M. *Inorg. Chem.* **1997**, 36, 3812. (k) Hirch, K. A.; Wilson, S. R.; Moore, J. S. *Inorg. Chem.* **1997**, 36, 2960; *J. Am. Chem. Soc.* **1997**, 119, 10401. (l) MacGillivray, L. R.; Subramanian, S.; Zaworotko, M. J. *J. Chem. Soc., Chem. Commun.* **1994**, 1325. (m) Robinson, F.; Zaworotko, M. *J. Chem. Soc., Chem. Commun.* **1995**, 2413.

[†] Universidad de Zaragoza.

[‡] Universidad de La Rioja.

(1) (a) Lehn, J. M. *Supramolecular Chemistry: Concept and Perspectives*; VCH: Weinheim, 1995. (b) Manners, I. *Angew. Chem., Int. Ed. Engl.* **1996**, 35, 1602. (c) Puddephatt, R. J. *Chem. Commun.* **1998**, 1055.

Scheme 1



$\{trans,trans,trans\text{-PtTl}_2(\text{C}_6\text{F}_5)_2(\text{C}\equiv\text{C}-t\text{-Bu})_2\}$ octahedral units^{7a} self-assembled by unusual secondary thallium-alkynyl (C_α) bonding interactions and a novel extended

platinum-silver compound $[\{\text{Pt}_2\text{Ag}_8(\text{C}\equiv\text{C}-t\text{-Bu})_8(\text{OCIO}_3)_2\text{S}_2\}(\text{O}_2\text{ClO}_2)_2]_\infty$ (S = acetone), **2**, containing 10-nuclear dicationic aggregate fragments connected through perchlorate bridging groups.^{7b} The synthesis of **2** was achieved by using the hexanuclear species $[\text{Pt}_2\text{Ag}_4(\text{C}\equiv\text{C}-t\text{-Bu})_8]$ (**1**) as precursor, which acts as an octadentate chelating bridging ligand in the final dicationic fragment through the external alkynyl coordination sites to four Ag^+ cations. Here, we report the synthesis and properties of two new platinum-silver polynuclear complexes (Scheme 1): an unexpected 1:1 cocrystallization adduct between the hexanuclear cluster **1** and the 2,2'-bipyridine ligand $[\{\text{Pt}_2\text{Ag}_4(\text{C}\equiv\text{C}-t\text{-Bu})_8(\text{bipy})\}]_\infty$ (**3**) and a new 10-

(3) Hydrogen bonds: (a) Desiraju, G. R. *Angew. Chem., Int. Ed. Engl.* **1995**, *35*, 2311. (b) Subramanian, S.; Zaworotko, M. J. *Coord. Chem. Rev.* **1994**, *137*, 357. (c) Burrows, A. D.; Chan, C. W.; Chowdhry, M. M.; McGrady, J. E.; Mingos, D. M. P. *Chem. Rev.* **1995**, *24*, 329. (d) Aakeröy, C. B.; Beatty, A. M. *Chem. Commun.* **1998**, 1067. (e) Aakeröy, C. B.; Beatty, A. M.; Leinen, D. S. *J. Am. Chem. Soc.* **1998**, *120*, 7383. $\text{M}\cdots\text{M}$ interactions: (f) Müller, J. S. *Extended Linear Chain Compounds*; Plenum Press: New York, 1982; Vols. 1–3. (g) Houlding, V. H.; Miskowski, V. M. *Coord. Chem. Rev.* **1991**, *91*, 1. (h) Williams, J. M. *Adv. Inorg. Chem. Radiochem.* **1983**, *26*, 235. (i) Aullón, G.; Alvarez, S. *Chem. Eur. J.* **1997**, *3*, 655. (j) Finnis, G. M.; Canadell, E.; Campana, Ch.; Dunbar, K. R. *Angew. Chem., Int. Ed. Engl.* **1996**, *35*, 2772, and references therein. (k) Connick, W. B.; Marsh, R. E.; Schaefer, W. P.; Gray, H. B. *Inorg. Chem.* **1997**, *36*, 913. (l) Daws, Ch. A.; Exstrom, Ch. L.; Sowa, J. R. Jr.; Mann, K. R. *Chem. Mater.* **1997**, *9*, 363. (m) Gliemann, G.; Yersin, H. *Struct. Bonding* **1985**, *62*, 87. (n) Mansour, M. A.; Connick, W. B.; Lachicotte, R. J.; Gysling, H. J.; Eisenberg, R. *J. Am. Chem. Soc.* **1998**, *120*, 1329. (o) Vickery, J. C.; Olmstead, M. M.; Fung, E. Y.; Balch, A. L. *Angew. Chem., Int. Ed. Engl.* **1997**, *36*, 1179. (p) Irwin, M. J.; Vittal, J. J.; Puddephatt, R. J. *Organometallics* **1997**, *16*, 3541. (q) Shieh, S. J.; Hong, X.; Peng, S. M.; Che, Ch. M. *J. Chem. Soc., Dalton Trans.* **1994**, 3067. (r) Tong, M.-L.; Cheng, X. M.; Ye, B.-H.; Ng, S. W. *Inorg. Chem.* **1998**, *37*, 5278. (s) Yamaguchi, T.; Yamazaki, F.; Tasuku, I. *J. Chem. Soc., Dalton Trans.* **1999**, 273. $\pi\cdots\pi$ interactions: (t) Munakata, M.; Wu, L. P.; Ning, G. L.; Kuroda-Sowa, T.; Maekawa, M.; Suenaga, Y.; Maeno, N. *J. Am. Chem. Soc.* **1999**, *121*, 4968, and references therein.

(4) (a) Lei, X.; Wolf, E. E.; Fehlner, T. P. *Eur. J. Inorg. Chem.* **1998**, 1835. (b) Jaito, T. *J. Chem. Soc., Dalton Trans.* **1999**, 97. (c) Liu, J.; Meyers, E. A.; Shore, S. G. *Inorg. Chem.* **1998**, *37*, 5410. (d) Prichard, R. G.; Parish, R. V.; Salehi, Z. *J. Chem. Soc., Dalton Trans.* **1999**, 243. (e) Burrows, A. D.; Mahon, M. F.; Palmer, M. T. *J. Chem. Soc., Dalton Trans.* **1998**, 1941. (f) Su, W.; Cao, R.; Hong, M.; Chen, J.; Lu, J. *Chem. Commun.* **1998**, 1389. (g) Hartshorn, C. M.; Steel, P. J. *J. Chem. Soc., Dalton Trans.* **1998**, 3935. (h) Yaghi, O. M.; Sun, Z.; Richardson, D. A.; Groy, T. L. *J. Am. Chem. Soc.* **1994**, *116*, 807. (i) Huang, Q.; Wu, X.; Wang, Q.; Sheng, T.; Lu, J. *Angew. Chem., Int. Ed. Engl.* **1996**, *35*, 868. (j) Lang, J. P.; Kawaguchi, H.; Tatsumi, K. *Inorg. Chem.* **1997**, *36*, 6447. (k) Campana, Ch.; Dunbar, K. R.; Onyang, X. *Chem. Commun.* **1996**, 2427.

(5) (a) Laine, R. M. *Inorganic and Organometallic Polymers with Special Properties*; Kluwer Academic Publishers: The Netherlands, 1992; p 331. (b) Weck, B.; Niemer, B.; Wieser, M. *Angew. Chem., Int. Ed. Engl.* **1993**, *32*, 923. For some recent works see: (c) Long, N. J.; Martin, A. J.; Vilar, R.; White, A. J. P.; Williams, D. J.; Younus, M. *Organometallics* **1999**, *18*, 4261, and references therein. (d) Chawdhury, N.; Köhler, A.; Friend, R. H.; Wong, W.-Y.; Lewis, J.; Younus, M.; Raithby, P. R.; Corcoran, T. C.; Al-Mandhary, M. R. A.; Khan, M. S. *J. Chem. Phys.* **1999**, *110*, 4963, and references therein. (e) Lavastre, O.; Even, M.; Dixneuf, P.; Pacreau, A.; Vairon, J. P. *Organometallics* **1996**, *15*, 1530. (f) See also: Hagihara, N.; Sonogashira, K.; Takahashi, S. *Adv. Polym. Sci.* **1981**, *41*, 149.

(6) (a) Brasse, C.; Raithby, P. R.; Rennie, M. A.; Russell, C. A.; Steiner, A.; Wright, D. S. *Organometallics* **1996**, *15*, 639. (b) Yamazaki, S.; Deeming, A. J.; Speel, D. M.; Hibbs, D. E.; Hursthouse, M. B.; Abdul Malik, K. M. *Chem. Commun.* **1997**, 177. (c) Guo, G.-C.; Wang, Q.-G.; Zhou, G.-D.; Mak, T. C. W. *Chem. Commun.* **1998**, 339. (d) Corfield, P. W. R.; Shearer, H. M. M. *Acta Crystallogr.* **1966**, *20*, 502. (e) Mingos, D. M. P.; Yan, J.; Menzer, S.; Williams, D. J. *Angew. Chem., Int. Ed. Engl.* **1995**, *34*, 1894. (f) Olbrich, F.; Kopf, J.; Weis, E. *Angew. Chem., Int. Ed. Engl.* **1993**, *32*, 1077.

(7) (a) Ara, I.; Berenguer, J. R.; Forniés, J.; Gómez, J.; Lalinde, E.; Merino, R. I. *Inorg. Chem.* **1997**, *36*, 6461. (b) Ara, I.; Forniés, J.; Gómez, J.; Lalinde, E.; Merino, R. I. Moreno, M. T. *Inorg. Chem. Commun.* **1999**, *2*, 62. (c) Chartmant, J. P. H.; Forniés, J.; Gómez, J.; Lalinde, E.; Merino, R. I.; Moreno, M. T.; Orpen, G. A. *Organometallics* **1999**, *18*, 3353.

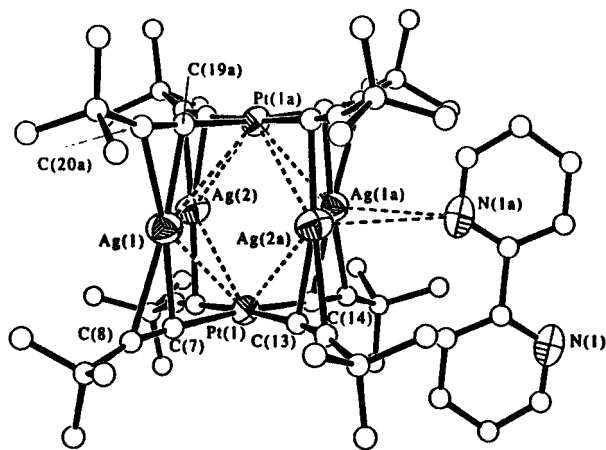


Figure 1. Repeating unit in $\{[Pt_2Ag_4(C\equiv C-t-Bu)_8(bipy)]\}_\infty$ (**3**) with the atom-numbering scheme. Carbon atoms are shown as spheres, and the hydrogen atoms have been omitted for clarity.

nuclear cationic species $\{[Pt_2Ag_4(C\equiv C-t-Bu)_8]\{Ag(bipy)\}_4\}-(ClO_4)_4$ (**4**). In **4**, the cluster $[Pt_2Ag_4(C\equiv C-t-Bu)_8]$ (**1**) acts as a base, being capped by four additional cationic Ag(bipy) units, and the 2,2'-bipy ligands adopt the very common chelating bonding mode.^{1a,8} In contrast, in the extended chain **3**, the octahedral $[Pt_2Ag_4(C\equiv C-t-Bu)_8]$ units seem to play the unusual role of a weak acid through the equatorial silver ions which are able to increase its coordination environment by unexpected misdirected long-range $Ag\cdots N$ contacts with bridging 2,2'-bipy ligand bridging four silver centers. Although a few crystal structures with bridging 2,2'-bipy are known,⁹ this interaction mode is completely unprecedented.

Results and Discussion

Synthesis and Structures. Treatment of $[Pt_2Ag_4(C\equiv C-t-Bu)_8]$ (**1**) with 2,2'-bipy (1:1 or 1:4 molar ratio) in acetone for 6 h produces a yellow-green solution from which the 1:1 adduct $\{[Pt_2Ag_4(C\equiv C-t-Bu)_8(bipy)]\}_\infty$ (**3**) is obtained as a yellow-green solid. Slow evaporation of a chloroform/hexane solution of **3** at room temperature produces yellow-green crystals of **3** in very high yield [72% (1:1) or 95% (1:4)] suitable for X-ray diffraction. Complex **3** crystallizes in the triclinic space group $P\bar{1}$ as an intriguing one-dimensional polymeric array extending along the crystallographic *b* axis. Figure 1 shows the repeating unit that comprises the hexanuclear cluster $[Pt_2Ag_4(C\equiv C-t-Bu)_8]$ and a very weakly interacting bipy ligand. Selected bond distances and angles are given in Table 1.

The most remarkable structural feature is that the formation of the final chain is controlled by the presence of 2,2'-bipyridine bridging ligands which are weakly contacting with the equatorial silver centers of adjacent cluster $[Pt_2Ag_4(C\equiv C-t-Bu)_8]$ units. The ability of 2,2'-

Table 1. Selected Bond Lengths (Å) and Angles (deg) for $\{[Pt_2Ag_4(C\equiv C-t-Bu)_8(bipy)]\}_\infty$ (**3**)

Pt(1)–C(13)	2.021(8)	Pt(1)–C(19)	2.025(7)
Pt(1)–C(7)	2.036(7)	Pt(1)–C(1)	2.046(7)
Pt(1)–Ag(2)	3.0039(6)	Pt(1)–Ag(1)	3.0595(6)
Pt(1)–Ag(2a)	3.2608(7)	Pt(1)–Ag(1a)	3.2722(7)
Ag(1)–C(7)	2.236(6)	Ag(1)–C(19a)	2.263(7)
Ag(1)–C(20a)	2.387(7)	Ag(1)–C(8)	2.562(7)
Ag(1)–Ag(2)	3.2627(9)	Ag(1)–Pt(1a)	3.2722(7)
Ag(1)–Ag(2a)	3.303(1)	Ag(2)–C(1)	2.227(9)
Ag(2)–C(13a)	2.219(8)	Ag(2)–C(14a)	2.402(8)
Ag(2)–C(2)	2.571(9)	Ag(2)–Pt(1a)	3.2608(7)
Ag(1)⋯N(1)	3.488	Ag(2)⋯N(1)	3.565
C(2)–C(1)–Pt(1)	171.1(8)	C(1)–C(2)–C(3)	168.8(9)
C(8)–C(7)–Pt(1)	174.7(6)	C(7)–C(8)–C(9)	167.3(8)
C(14)–C(13)–Pt(1)	172.8(7)	C(13)–C(14)–C(15)	167.7(9)
C(20)–C(19)–Pt(1)	175.3(7)	C(19)–C(20)–C(21)	161.4(7)

bipyridine to act as a chelating ligand (*endo*-bidentate) is well established.^{1a,8} However, species with bridging bipyridines are rather rare. Some examples have been proposed on the basis of indirect evidence,¹⁰ but, as far as we know, only a few crystal structures of binuclear complexes (Cr, Pt, Pd) are known.⁹ To the best of our knowledge, this is the first example reported in an extended structure. As in the free ligand,¹¹ the bipy is planar, with a dihedral angle of 180° between both pyridine rings, and assumes an *s-trans* conformation imposed by a crystallographic inversion center. Although both *cisoidal*^{9a,c,d} and *transoidal*^{9b} arrangements have been previously observed, the planar conformation contrasts with the nonplanar forms previously found in the above binuclear μ -bipy complexes,⁹ although in this case the interactions between the silver centers of the cluster and the bipy ligand are nearly negligible. Each nitrogen atom of the bipy ligand displays very long misdirected contacts of 3.488 and 3.565 Å with two adjacent silver equatorial atoms of the cluster unit, and the bipy molecules act as μ_4 -bridging ligands in the final network. These distances are slightly longer than the sum of the van der Waals radii (3.25 Å) and are comparable with that reported [3.439(2) Å] in $[Ag\{P(CH_2CH_2CN)_3\}_2]NO_3$, in which the silver atom is encapsulated by the six CN groups.¹² However, despite their weakness, these contacts control the structural conformation of the platinum fragments within the cluster and their emissive properties. Thus, the most remarkable difference of the cluster building block $[Pt_2Ag_4(C\equiv C-t-Bu)_8]$ in the adduct **3** in relation to the free cluster **1**¹³ is the eclipsed orientation of the two square-planar $Pt(C\equiv C-t-Bu)_4$ fragments within the octahedral cluster [torsion angle C(7)–Pt(1)–Pt(1a)–C(19a) 0.5°], which were observed to be clearly staggered in **1** [torsion angles 37.13(12)° and 32.84(5)°]. The remaining structural details are rather similar to those observed in **1**, although perhaps a little more asymmetrical. Thus, two

(8) (a) Martell, A. E.; Hancock, R. D. *Metal Complexes in Aqueous Solutions*; Plenum: New York, 1996. (b) Zelewsky, A. V. *Stereochemistry of Coordination Compounds*; Wiley: Chichester, 1996.

(9) (a) van Belzeu, R.; Klein, R. A.; Kooijman, H.; Veldman, N.; Spek, A. L.; Elsevier, C. J. *Organometallics* **1998**, *17*, 1812. (b) Usón, R.; Forníés, J.; Tomás, M.; Martínez, F.; Casas, J. M.; Fortuño, C. *Inorg. Chim. Acta* **1995**, *235*, 51. (c) Forníés, J.; Navarro, R.; Sicilia, V.; Tomás, M. *Inorg. Chem.* **1993**, *32*, 3675. (d) Creaven, B. S.; Long, C.; Howie, R. A.; McQuillan, G. P.; Low, J. *Inorg. Chim. Acta* **1989**, *157*, 151.

(10) (a) Lawson, D. N.; Wilkinson, G. *J. Chem. Soc.* **1965**, 1900. (b) Mufti, A. S.; Poller, R. C. *J. Organomet. Chem.* **1965**, *3*, 99. (c) Komura, M.; Kawasaki, Y.; Tanaka, T.; Okawara, R. *J. Organomet. Chem.* **1965**, *4*, 308. (d) Matsubayashi, G. *J. Inorg. Nucl. Chem.* **1996**, *28*, 2937. (e) Fowles, G. W. A.; Willey, G. R. *J. Chem. Soc.* **1968**, 1435. (f) Cuenca, T.; Royo, P. *J. Organomet. Chem.* **1985**, *293*, 61.

(11) Merryt, L. L., Jr.; Schröder, E. D. *Acta Crystallogr.* **1956**, *9*, 801.

(12) Liu, C. W.; Pan, H.; Fackler, J. P.; Wu, G.; Wasylishen R. E.; Shang, M. *J. Chem. Soc., Dalton Trans.* **1995**, 3691.

(13) Espinet, P.; Forníés, J.; Martínez, F.; Tomás, M.; Lalinde, E.; Moreno, M. T.; Ruiz, A.; Welch, A. J. *J. Chem. Soc., Dalton Trans.* **1990**, 791.

Pt...Ag distances are approximately 0.23 Å longer than the other two [Pt(1)–Ag(1,2) 3.0595(6), 3.0039(6) Å vs Pt(1)–Ag(1a,2a) 3.2722(7), 3.2608(7) Å], and the Ag(1)–Ag(2) separation [3.2627(9) Å] is slightly shorter than the unbridged distance Ag(1)–Ag(2a) [3.303(1) Å]. Although all these distances are shorter than twice the van der Waals limit (3.4–3.6 Pt, 3.4 Ag),¹⁴ only weak metal...metal interactions (if any) are probably present. Although several examples of platinum–silver complexes containing unsupported Pt(II)–Ag dative bonds of lengths of about 3.0 Å have been described,^{3s,15} in this cluster the presence of an alkynyl bridging ligand probably has a significant effect on the Pt...Ag distance. The η^2 -alkynyl–silver bond distances [Ag–C _{α} 2.219(8)–2.263(7); Ag–C _{β} 2.387(7)–2.571(9) Å] and the geometrical details of the alkynyl ligands are unremarkable within this type of complexes.^{7b,13,16} The IR spectrum of crystals of **3** (KBr pellets) contains essentially the same bands as those found in the free cluster **1** and bipy ligand [$\nu(\text{C}\equiv\text{C})$ 2044 **3** vs 2043 **1** in KBr]. However, although the crystallographic study confirms the aggregation in the solid state, as expected, this is not the case in solution. Its proton spectrum in CDCl₃ showed the resonances due to bipy in the aromatic region (8.68, 8.39, 7.82, and 7.31 ppm) and the presence of a single *tert*-butyl resonance due to the alkynyl fragments of cluster (δ 1.30) in the expected ratio. Both types of resonances appear at a chemical shift similar to those observed in free **1** and the ligand, indicating that the aggregation process is not occurring in solution. After prolonged accumulation, its ¹³C NMR spectrum also exhibits signals that can be attributed to bipy and free cluster **1** (see Experimental Section).

Attempts to obtain a similar adduct with the copper cluster [Pt₂Cu₄(C≡C-*t*-Bu)₈] failed, since following a procedure (1:1 molar ratio) similar to that described for **3**, only crystals of the starting material separated. The lack of reactivity of these clusters toward the chelating 2,2'-bipy suggests a notable stability of these [Pt₂M₄(C≡C-*t*-Bu)₈] clusters and a higher coordinating ability of the alkynyl fragments toward Cu(I) or Ag(I) compared to the bipy ligand in these systems. The stability toward the 2,2'-bipy ligand is interestingly high compared to that previously observed toward anionic or neutral ligands.¹⁷ This result prompted us to explore the reactivity of **2**, prepared by reaction of **1** with an excess of AgClO₄, toward the 2,2'-bipy ligand. The formulation of **2** as a polymeric chain [$\{\text{Pt}_2\text{Ag}_8(\text{C}\equiv\text{C}-t\text{-Bu})_8(\text{OClO}_3)_2(\text{acetone})_2(\text{O}_2\text{ClO}_2)_2\}_n$ (**2**) was established by X-ray crystallography on crystals obtained from acetone/hexane.^{7b} The reaction was studied in different molar ratios (see Scheme 1).

The 4:1 (bipy:2) reaction in acetone yielded [1{Ag(bipy)}₄](ClO₄)₄ (**4**), which precipitates in the reaction

(14) Huheey, J. E.; Keiter, E. A.; Keiter, R. A. *Inorganic Chemistry*, 4th ed.; Harper Collins Publishers: 1993; p 292.

(15) (a) Aullón, G.; Alvarez, S. *Inorg. Chem.* **1996**, *35*, 3137. (b) Forniés, J.; Martín, A. in *Metal Clusters in Chemistry*; Braunstein, P.; Oro, L. A.; Raithby, P. R. Eds.; Wiley-VCH: New York, 1999; Vol. 1, Chapter 22.

(16) (a) Espinet, P.; Forniés, J.; Martínez, F.; Sotés, M.; Lalinde, E.; Moreno, M. T.; Ruiz, A.; Welch, A. J. *J. Organomet. Chem.* **1991**, *403*, 253. (b) Forniés, J.; Lalinde, E.; Martínez, F.; Moreno, M. T.; Welch, A. J. *J. Organomet. Chem.* **1993**, *455*, 271. (c) Forniés, J.; Gómez-Saso, M. A.; Martínez, F.; Lalinde, E.; Moreno, M. T.; Welch, A. J. *New J. Chem.* **1992**, *16*, 483.

(17) Forniés, J.; Lalinde, E.; Martín, A.; Moreno, M. T. *J. Organomet. Chem.* **1995**, *490*, 179.

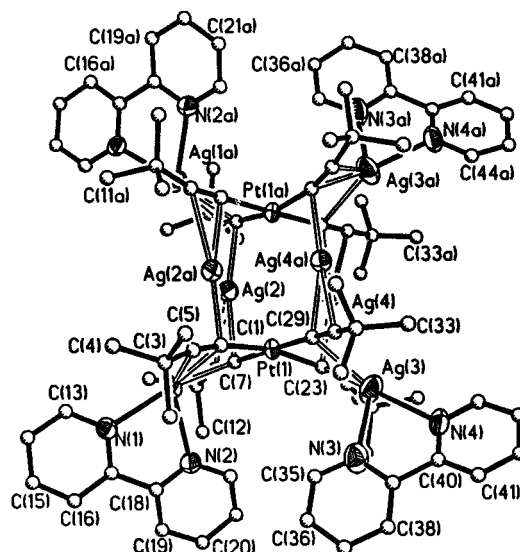


Figure 2. Molecular structure of the ion [$\{\text{Pt}_2\text{Ag}_4(\text{C}\equiv\text{C}-t\text{-Bu})_8\}\{\text{Ag}(\text{bipy})_4\}^{4+}$ of **4** showing the atom-numbering scheme. Carbon atoms are shown as spheres, and the hydrogen atoms have been omitted for clarity.

mixture as a yellow solid. Recrystallization from chloroform/hexane afforded **4** in the form of yellow needles, some of which were adequate for an X-ray crystallography study (see below). The 8:1 and 6:1 (bipy:2) reactions in acetone yielded pale yellow solutions, from which a microcrystalline very pale yellow compound of stoichiometry [Pt₂Ag₈(C≡C-*t*-Bu)₈(bipy)₆](ClO₄)₄ (**5**) was isolated. Both **4** and **5** exhibit in their IR spectra, in addition to bands due to $\nu(\text{C}\equiv\text{C})$ [2023 (w) cm⁻¹ **4**; 2047 (w), 2010 (m) cm⁻¹ **5**] and bipy ligands, the typical absorptions of uncoordinated ClO₄⁻ anions¹⁸ [1087, 622 **4**; 1092, 621 cm⁻¹ **5**]. The most remarkable difference is found in their proton spectra, both in the alkynyl resonances (δ 1.17 **4**; δ 1.23 **5**) and in the bipy signals [9.11 (s, br), 8.37 (d), 8.14 (st), 7.52 (st) **4** vs 8.80 (s, br), 8.33 (d), 8.00 (st), 7.49 (st) **5**]. In the ¹³C NMR spectrum of complex **4**, only the signals due to bipy and *t*-Bu groups can be observed, due probably to its very low solubility in CDCl₃ (see Experimental Section). The solubility of **5** is extremely low for ¹³C NMR studies. Its structure remains uncertain. Although this complex crystallizes easily in different solvent systems, we have not been able to obtain good crystallographic results. In one instance we noted that, by slow diffusion of hexane into a chloroform solution of complex **5**, crystals of the adduct [1·bipy]_∞ (**3**) were formed, as confirmed by X-ray crystallography, thus suggesting the remarkable stability of this species. The formulation, shown in Scheme 1, is tentatively assigned on the basis of (i) its molar conductivity (472 Ω⁻¹ cm² mol⁻¹), which is in the expected range for 1:4 electrolytes in nitromethane solution, as for complex **4** (344 Ω⁻¹ cm² mol⁻¹), and (ii) the presence of two different $\nu(\text{C}\equiv\text{C})$ absorptions in the solid state in its IR spectrum.

The structure of the cation of **4** is shown in Figure 2, and selected interatomic distances and angles are listed in Table 2. The cation in **4** can be considered as being derived from that of the dicationic fragment building

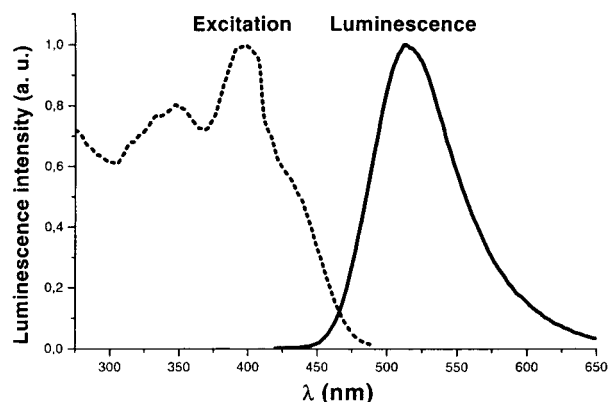
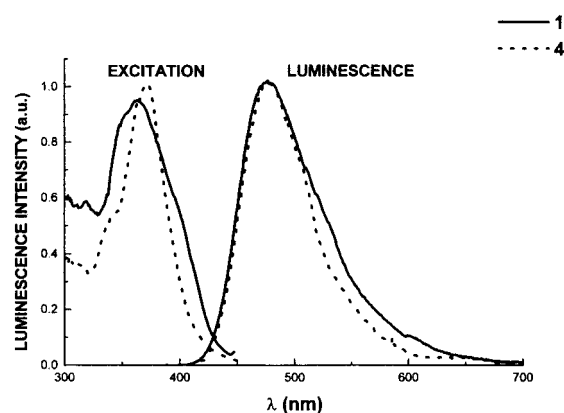
(18) Nakamoto, K. *Infrared and Raman Spectra of Inorganic and Coordination Compounds*; Wiley: New York, 1986.

Table 2. Selected Bond Lengths (Å) and Angles (deg) for the Cation $[\{Pt_2Ag_4(C\equiv C-t-Bu)_8\}\{Ag(bipy)\}_4]^{4+}$ in **4**

Pt(1)–C(29)	2.02(1)	Pt(1)–C(1)	2.02(1)
Pt(1)–C(7)	2.04(1)	Pt(1)–C(23)	2.04(1)
Pt(1)–Ag(4)	3.0172(9)	Pt(1)–Ag(2a)	3.057(1)
Pt(1)–Ag(2)	3.160(1)	Pt(1)–Ag(4a)	3.217(1)
Pt(1)–Ag(3)	3.238(1)	Pt(1)–Ag(1)	3.280(1)
Ag(1)–N(1)	2.322(9)	Ag(1)–C(1)	2.38(1)
Ag(1)–N(2)	2.378(9)	Ag(1)–C(7)	2.57(1)
Ag(1)–C(2)	2.61(1)	Ag(2)–C(1a)	2.22(1)
Ag(2)–C(7)	2.28(1)	Ag(2)–C(8)	2.49(1)
Ag(2)–Ag(2a)	3.177(2)	Ag(2)–Ag(4)	3.309(1)
Ag(3)–N(4)	2.305(9)	Ag(3)–C(23)	2.364(9)
Ag(3)–N(3)	2.38(1)	Ag(3)–C(29)	2.54(1)
Ag(3)–C(24)	2.58(1)	Ag(4)–C(23)	2.25(1)
Ag(4)–C(29a)	2.26(1)	Ag(4)–C(30a)	2.50(1)
Ag(4)–Ag(4a)	3.141(2)	C(1)–C(2)	1.22(2)
C(7)–C(8)	1.22(2)	C(23)–C(24)	1.21(2)
C(29)–C(30)	1.22(2)		
C(29)–Pt(1)–C(1)	85.9(4)	C(1)–Pt(1)–C(7)	94.0(4)
C(29)–Pt(1)–C(23)	93.6(4)	C(7)–Pt(1)–C(23)	86.2(4)
N(1)–Ag(1)–N(2)	71.2(3)	C(1)–Ag(1)–C(7)	73.7(3)
N(4)–Ag(3)–N(3)	71.2(3)	C(23)–Ag(3)–C(29)	74.0(3)
Ag(4a)–Ag(4)–Ag(2)	90.04(2)	C(2)–C(1)–Pt(1)	166(1)
C(2)–C(1)–Ag(2a)	100.0(8)	C(2)–C(1)–Ag(1)	86.8(8)
C(1)–C(2)–C(3)	169(2)	C(8)–C(7)–Pt(1)	175.2(9)
C(8)–C(7)–Ag(2)	85.0(8)	C(8)–C(7)–Ag(1)	94.6(7)
C(7)–C(8)–C(9)	168(2)	C(24)–C(23)–Pt(1)	168.6(9)
C(24)–C(23)–Ag(4)	101.1(8)	C(23)–C(24)–C(25)	172(2)
C(23)–C(24)–Ag(3)	66.1(7)	C(30)–C(29)–Pt(1)	174.0(9)
C(30)–C(29)–Ag(4a)	86.2(8)	C(30)–C(29)–Ag(3)	93.0(8)
C(29)–C(30)–C(31)	169(1)		

block of **2** (see Scheme 1) with replacement of bridging and terminal perchlorate and acetone ligands on each external silver center by a chelating 2,2'-bipy ligand. Thus, the central hexanuclear cluster is acting as an octadentate bridging ligand being tetracapped by four external cationic Ag(bipy) units. Within the hexanuclear cluster both tetraalkynylplatinate(II) moieties exhibit an essentially eclipsed conformation (torsion angle 0.8°). Although the internal silver centers [Ag(2), Ag(4)] are dicoordinated by two alkyne entities (one from each Pt fragment) as in **1**, **2**, or **3**, their interaction with the alkynyl fragments is somewhat different, being η^2 -bonded to one and $\eta^1(C_\alpha)$ -bonded to the other. The external silver centers [Ag(1), Ag(3)] are chelated by a bipy ligand [Ag–N 2.305(9)–2.38(1) Å] and complete a four-coordinated strongly distorted environment, midway between a tetrahedral and pyramidal trigonal coordination sphere, interacting with two mutually *cis* alkynyl ligands (η^2 -bonded to one C≡C fragment and η^1 -bonded to the C_α atom of the other). As a consequence, each alkynyl ligand exhibits an unsymmetrical μ_3 - η^2 coordination mode (σ -Pt, η^2 -Ag, η^1 -Ag). The interaction of the alkynyl ligands with the external Ag centers is clearly weaker [Ag– C_α 2.364(9)–2.57(1) Å; Ag– C_β 2.58(1)–2.61(1) Å] than with the internal ones [Ag– C_α 2.22(1)–2.28(1) Å; Ag– C_β 2.49(1)–2.50(1) Å]. The Pt⋯Ag distances observed within the central hexanuclear cluster core are slightly shorter [3.0172(9)–3.217(1) Å] than the external Pt⋯Ag separations [3.238(1)–3.280(1) Å] and comparable with those observed in **1**–**3**. The Ag⋯Ag distances range from 3.141(2) Å for Ag(4)–Ag(4a) to 3.309(1) Å for Ag(2)–Ag(4), all being considered as nonbonding interactions.

Excitation and Emission Spectra. All complexes are luminescent in the solid state and in frozen solutions (acetone, 77 K), but luminescence is not detected in

**Figure 3.** Excitation and emission spectra of $[\{Pt_2Ag_4(C\equiv C-t-Bu)_8(bipy)\}]_\infty$ (**3**) in the solid state (KBr pellets) at room temperature.**Figure 4.** Excitation and emission spectra of $[Pt_2Ag_4(C\equiv C-t-Bu)_8]$ **1** (—) and $[\{Pt_2Ag_4(C\equiv C-t-Bu)_8\}\{Ag(bipy)\}_4](ClO_4)_4$ **4** (---) in the solid state (KBr pellets) at room temperature.

solution at room temperature. Figures 3 (complex **3**) and 4 (complex **4**) show their room-temperature excitation and emission spectra together with those of the cluster precursor **1** and are included in Figure 4 for comparison.

As can be observed (Figure 4), the 10-nuclear derivative $[\{Pt_2Ag_4(C\equiv C-t-Bu)_8\}\{Ag(bipy)\}_4](ClO_4)_4$ (**4**) displays a luminescence similar to that observed for the hexanuclear cluster $[Pt_2Ag_4(C\equiv C-t-Bu)_8]$ (**1**), thus suggesting that the influence of the four external Ag(bipy) units on the central hexanuclear chromophore is negligible. In both cases, excitation at different λ within the absorption spectra ($\lambda_{abs,max}$ 370, 343 (sh), 303, 261 **1**; 376, 300 **4** in KBr) results in an intense emission slightly more asymmetric for **1** with a maximum at 476 nm. The excitation spectra show narrow features centered at 365 nm for **1** and at 370 nm for **4**, which match well with the lowest energy absorption bands. On the basis of its large Stoke's shift (6389 cm^{-1} **1**, 6019 cm^{-1} **4**) and relatively long lifetime (nonexponential decay with a short component of $0.35\ \mu\text{s}$), the emission observed is assigned to a phosphorescence. However, complex **5**, $[Pt_2Ag_8(C\equiv C-t-Bu)_8(bipy)_6](ClO_4)_4$, exhibits a red-shifted luminescence band (1666 cm^{-1}) with respect to that of **1** ($\lambda_{emis,max}$ 517 nm, $\lambda_{exc,max}$ 429, 390, 347, 306 nm). In a recent communication and on the basis of previous spectroscopic reports, we tentatively ascribed the emission of **1** to a ligand (acetylide) to metal cluster core charge transfer ($C\equiv C-t-Bu \rightarrow Pt_2Ag_4$). As mentioned in

Table 3. Summary of Computational Results for [Pt₂Ag₄(C≡C-*t*-Bu)₈] (1) and [Pt(C≡C-*t*-Bu)₄]²⁻

compound	HOMO [E(eV)]	LUMO [E(eV)]
[Pt ₂ Ag ₄ (C≡C- <i>t</i> -Bu) ₈], 1	π^* Pt($d_{x^2-y^2}$, d_{xy} , 54%) - π_{xy} (C≡C) -11.8	Pt(p_z 20%) - Ag(sp 24%) - C _{β} (p_z 56%) -8.5
[Pt(C≡C- <i>t</i> -Bu) ₄] ²⁻	π^* Pt($d_{x^2-y^2}$ 58%) - π_{xy} (C≡C- <i>t</i> -Bu) -11.8	Pt(p_z 31%) - π^* (C≡C) (p_z) -7.6

a second report dealing with unusual properties of the trimer complex [Pt₂Cu₄(C≡CPh)₈]₃, the red shift observed for the analogous phenyl derivative [Pt₂Ag₄(C≡CPh)₈] (yellow form λ_{\max} 570 nm) was in agreement with this assignment. The higher emission energy of **1** in relation to [Pt₂Ag₄(C≡CPh)₈] is in keeping with the increasing π^* orbital energy of the acetylide ligand, supporting the involvement of the π^* (C≡CR) orbitals in the transition. With the aim to know qualitatively the origin of the emission EHMO,¹⁹ computations were performed on the cluster **1**. The analysis was carried out using the interactions between two [Pt(C≡C-*t*-Bu)₄]²⁻ fragments with the four Ag⁺ centers (*D*₄ symmetry). The overall results provide an approximate description of the nature of the frontier MO and are presented in Table 3. Qualitatively the HOMO originates in a π filled–filled type interaction analogous to that previously reported for more simple alkynyl complexes. The HOMO is a π^* orbital with platinum (54%) and carbon (46%) character which arises from a π interaction between orbitals of the platinum centers [$d_{x^2-y^2}$ Pt(1); d_{xy} Pt(2)] and the π_{xy} (C≡C) orbital of the alkynyl fragments. The character of this orbital is rather similar to the HOMO in the [Pt(C≡C-*t*-Bu)₄]²⁻ fragment (*C*_{4v} symmetry, Pt: 5d _{x^2-y^2} 58%, π_{xy} (C≡C) 42%). In contrast, while the LUMO in [Pt(C≡C-*t*-Bu)₄]²⁻ is localized within the π^* C≡C (p_z) system with a substantial mixing with the 6 p_z orbital of Pt (see Table 3), in cluster **1**, there is also a significant participation of the valence orbitals of Ag centers. The LUMO orbital is a nonbonding orbital with contributions of silver (24% sp), platinum (20% p_z), and mainly the carbon atom C _{β} (56%) of the C≡C fragment. According to this analysis, since the Pt d character in the HOMO is higher than the Pt p_z in the LUMO and there is a notable participation of Ag orbitals in the latter, a Pt₂ → Pt₂Ag₄(C≡C-*t*-Bu)₈ charge transfer (MLMCT) would be appropriate for the transition.

The emission properties of polymer chain [1·bipy]_∞ (**3**) show clear evidence of the misdirected interactions between the 2,2'-bipy ligand and the equatorial Ag centers of the cluster. This complex exhibits a very intense luminescence which is red-shifted (1515 cm⁻¹) with respect to that of **1** ($\lambda_{\text{em,max}}$ 513 nm **3** vs 476 nm **1**). We estimate that the solid-state luminescence of **3** is at least 3 times higher than that of the free cluster **1**. In addition to this, the excited state lifetime of **3** is significantly longer ($\tau = 13 \mu\text{s}$) than that found for **1** (0.35 μs). The difference in $\lambda_{\text{emis,max}}$ between **1** and **3** suggests that very weak interactions between **1** and 2,2'-bipy may indeed play a role in the stabilization energy of the emissive state.²⁰ In fact, the excitation maximum for **3** is also red shifted [λ_{exct} 398 nm, 433 (sh)] from that observed for **1**. On the other hand, the higher luminescence and longer lifetime suggest a substantial

reduction in the overall deactivation nonradiative mechanism. The existence of misdirected interactions between the 2,2'-bipy ligand and the equatorial silver centers of the clusters seems to cause a slight stabilization of the emitting state and to prevent access to the ground state through other nonradiative deactivation processes, probably reducing the vibrational overlap between the emitting and ground state.

In summary, this study illustrates not only the possibility of using the 2,2'-bipy as connecting ligand in extended structures but also the possibility of performing a fine-tuning of the optical properties of these species by varying the connecting bridging group of the clusters, the substituent alkynyl ligand, and the metal center implicated in the η^2 -interactions. Work in this direction is now in progress.

Experimental Section

Elemental analyses were carried out with a Perkin-Elmer 2400 CHNS/O microanalyzer, the electrospray mass spectra on a HP5989B with interphase API-ES HP59987A, and the mass spectra (FAB+) on a VG Autospec spectrometer. Conductivities of nitromethane solutions in ca. 5×10^{-4} mol L⁻³ solutions were measured with a Crison GLP 31 conductimeter. IR spectra were recorded on a Perkin-Elmer FT-IR 1000 spectrometer and NMR spectra on a Bruker ARX 300 spectrometer [chemical shifts are reported in ppm relative to external standards (SiMe₄) and *J* in Hz]. The starting complexes [Pt₂Ag₄(C≡C-*t*-Bu)₈]¹³ and [(Pt₂Ag₈(C≡C-*t*-Bu)₈)(OCIO₃)₂(acetone)₂](O₂ClO₂)₂∞^{7b} were prepared as described elsewhere. The absorption spectra were registered in an UV–vis Hitachi U-3400 (solid) spectrophotometer. Luminescence, as well as excitation spectra for **3** and **5**, was registered on a Perkin-Elmer luminescence spectrometer LS 50B with a red-sensitive photomultiplier type R928, and for **1** and **4** a standard calibrated tungsten–halogen lamp was used (the spectra have been corrected). The lifetime was measured using a pulsed EG&G (**1**, **2**) dye laser or a Perkin-Elmer luminescence spectrometer LS 50B (**3**).

Preparation of [(Pt₂Ag₄(C≡C-*t*-Bu)₈(bipy)]_∞ (3**).** A mixture of [Pt₂Ag₄(C≡C-*t*-Bu)₈] (**1**) (0.100 g, 0.061 mmol) and 2,2'-bipyridine (0.038 g, 0.246 mmol) was stirred in acetone for 6 h. The resulting solution was evaporated to dryness, giving a yellow-green solid, which was dissolved in a mixture of CHCl₃/hexane. By slow evaporation of the solution at room temperature, yellow-green crystals began to grow. After several days, the crystals were separated by filtration, washed with *n*-hexane, and air-dried (0.104 g, 95% yield). By using a stoichiometric amount of 2,2'-bipy ligand (cluster:bipy 1:1), the yield was reduced to 72%. Anal. Calcd for Ag₄C₅₈H₈₀N₂Pt₂: C, 38.99; H, 4.51; N, 1.57. Found: C, 39.21; H, 5.02; N, 1.36. MS (FAB+): *m/z* 1579 ([1]Ag⁺, 60), 1471 ([Pt₂Ag₄(C≡C-*t*-Bu)₈+1]⁺, 20), 1309 ([Pt₂Ag₄(C≡C-*t*-Bu)₆+1]⁺, 35), 1227 ([Pt₂-Ag₄(C≡C-*t*-Bu)₅]⁺, 100), 1146 ([Pt₂Ag₄(C≡C-*t*-Bu)₄]⁺, 60), peaks at 2210 (15%), 1721 (20%), 1009 (30%), 899 (85%) and 791 (45%) are also observed. es(-): *m/z* 696 ([Ag₂(C≡C-*t*-Bu)₄bipy], 48), 531 ([Ag₂(C≡C-*t*-Bu)₂bipy-3], 21). IR (KBr, ν_{max} /cm⁻¹): 2044 (s) (C≡C), 1583 (m), 1560 (m), 1144 (w), 1069 (w), 762 (s) (bipy), 542 (s) (Pt–C). ¹H NMR (CDCl₃): δ 8.68 (s) (H₃₃), 8.39 (d, *J* = 1.5 H₆₆), 7.82 (st, *J* = 7.6 H₅₅), 7.31 (m, H₄₄) (bipy), 1.30 (s, *t*-Bu). ¹³C NMR (CDCl₃): δ 148.95, 136.72, 123.50

(19) Mealli, C.; Proserpio, D. M. *J. Chem. Educ.* **1990**, *67*, 399.

(20) It should be noted that the free bipy ligand exhibits an extremely weak emission at $\lambda_{\text{max}} = 537$ nm ($\lambda_{\text{exct}} = 348$ nm).

Table 4. Crystal Data and Structure Refinement Parameters for **3** and **4**

	3	4
empirical formula	C ₉₆ H ₁₃₂ Ag ₆ N ₂ Pt ₂	C ₈₈ H ₁₀₄ Ag ₈ Cl ₄ N ₈ O ₁₆ Pt ₂
fw	2351.44	2924.73
temperature	293(2) K	200(2) K
wavelength	0.71073 Å	0.71073 Å
cryst syst	triclinic	monoclinic
space group	<i>P</i> 1	<i>C</i> 2/ <i>c</i>
unit cell dimens	<i>a</i> = 10.892(3) Å <i>b</i> = 11.861(3) Å <i>c</i> = 12.778(3) Å α = 73.86(1)° β = 77.35(1)° γ = 87.24(1)°	<i>a</i> = 14.929(1) Å <i>b</i> = 22.985(3) Å <i>c</i> = 29.596(3) Å α = 90° β = 91.72(1)° γ = 90°
volume	1547.05(7) Å ³	10151(2) Å ³
<i>Z</i>	1	4
calcd density	2.524 Mg/m ³	1.914 Mg/m ³
abs coeff	6.424 mm ⁻¹	4.419 mm ⁻¹
<i>F</i> (000)	1160	5664
cryst size	0.40 × 0.35 × 0.30 mm	0.40 × 0.40 × 0.18 mm
θ range for data collection	3.07–29.14°	2.10–25.01°
limiting indices	–14 ≤ <i>h</i> ≤ 14 –15 ≤ <i>k</i> ≤ 16 –16 ≤ <i>l</i> ≤ 17	–1 ≤ <i>h</i> ≤ 17 –1 ≤ <i>k</i> ≤ 27 –35 ≤ <i>l</i> ≤ 35
no. of reflns collected	12 324	10 555
no. of ind reflns	8226 [<i>R</i> (int) = 0.0553]	8896 [<i>R</i> (int) = 0.0412]
refinement method	full-matrix least-squares on <i>F</i> ²	
no. of data/restraints/params	8226/0/310	7860/0/550
goodness-of-fit on <i>F</i> ^{2a}	1.214	1.025
final <i>R</i> indices [<i>I</i> > 2σ(<i>I</i>)] ^b	<i>R</i> 1 = 0.0534, <i>wR</i> 2 = 0.1407	<i>R</i> 1 = 0.0521, <i>wR</i> 2 = 0.0925
<i>R</i> indices (all data)	<i>R</i> 1 = 0.0662, <i>wR</i> 2 = 0.1579	<i>R</i> 1 = 0.1091, <i>wR</i> 2 = 0.1125
largest diff peak and hole	1.329 and –1.825 e·Å ⁻³	1.117 and –0.699 e·Å ⁻³

^a Goodness-of-fit = $[\sum w(F_o^2 - F_c^2)^2 / (n_{\text{obs}} - n_{\text{param}})]^{1/2}$. *w* = $[o^2(F_o) + (g_1P)^2 + g_2P^{-1}]^{-1}$; *P* = $[\max(F_o^2, 0) + 2F_c^2]/3$. ^b *R*1 = $\sum(|F_o| - |F_c|) / \sum|F_o|$; *wR*2 = $[\sum w(F_o^2 - F_c^2)^2 / \sum w(F_c^2)^2]^{1/2}$.

(bipy), 120.79 (bipy and C_β, C≡C-*t*-Bu), 71.00 (C_α, C≡C-*t*-Bu), 32.91 [s, C(CH₃)₃], 29.92 [s, C(CH₃)₃].

The ¹³C NMR spectra of bipy (δ 155.70, 148.79, 136.52, 123.34, 120.66) and [Pt₂Ag₄(C≡C-*t*-Bu)₈] [120.69 (s, ²*J*_{Pt-C_β} = 298.7 Hz, C_β, C≡C-*t*-Bu), 71.06 (s, ¹*J*_{Pt-C_α} = 894 Hz, C_α, C≡C-*t*-Bu), 32.92, 32.89 (C(CH₃)₃), 29.90 (s, C(CH₃)₃)] in CDCl₃ have been registered for comparison.

Preparation of [(Pt₂Ag₄(C≡C-*t*-Bu)₈)]₄(ClO₄)₄, **4.** To a stirred suspension of [(Pt₂Ag₆(C≡C-*t*-Bu)₈](ClO₄)₂·(acetone)₂(O₂ClO₂)₂·**2** (0.150 g, 0.065 mmol) in acetone (10 mL) was added a solution of 2,2'-bipy (0.0407 g, 0.261 mmol) in the same solvent (20 mL). A yellow solution was immediately obtained, and after a few minutes of stirring, a yellow solid began to precipitate. The mixture was stirred for 12 h, and the resulting precipitate was collected by filtration and washed with acetone. Evaporation of the filtrate gave a second fraction of solid. Crystallization of both solids (identical by NMR spectroscopy) from CHCl₃/hexane yielded **4** as microcrystalline yellow needles. Overall yield ≈ 55%. Anal. Calcd for Ag₈C₈₈Cl₄H₁₀₄N₈O₁₆Pt₂: C, 36.14; H, 3.58; N, 3.83. Found: C, 35.99; H, 2.98; N, 4.20. MS FAB(+): *m/z* 1785 ([Pt₂Ag₆(C≡C-*t*-Bu)₈(ClO₄)₂]⁺, 36), 1579 ([**1**Ag]⁺, 100), 1255 ([Pt₂Ag₂(C≡C-*t*-Bu)₈]⁺, 27), peaks at 1852 (15%), 1009 (35%) and 899 (15%) are also observed. A peak at *m/z* 3046 is tentatively assigned to [(**1**)₂Ag]⁺. *es*(+): *m/z* 1787 ([Pt₂Ag₆(C≡C-*t*-Bu)₈(ClO₄)₂]⁺, 100), 1578 ([**1**Ag-1]⁺, 49), 1255 ([Pt₂Ag₂(C≡C-*t*-Bu)₈]⁺, 50), 421 ([Ag(bipy)₂+2]⁺, 63). Λ_M (in nitromethane solution): 344 Ω⁻¹ cm² mol⁻¹. IR (Nujol, ν_{max} /cm⁻¹): 2023 (w) (C≡C), 1087 (vs,br), 622 (vs) (ClO₄⁻ stretching and bending), 1593 (s), 1565 (w), 780 (sh), 764 (vs) (bipy). ¹H NMR (CDCl₃): δ 9.11 (s, br), 8.37 (d, *J* = 7.9), 8.14 (st, *J* ≈ 7.4), 7.52 (st, *J* ≈ 5.8) (bipy), 1.17 (s, *t*-Bu). ¹³C NMR (CDCl₃): δ 151.03, 150.92, 139.60, 125.85, 122.63 (bipy), 32.55, 32.51 [C(CH₃)₃], 30.36 [s, C(CH₃)₃]. The signals due C_α and C_β carbon atoms are not observed due to the low solubility of the complex.

Preparation of [Pt₂Ag₈(C≡C-*t*-Bu)₈(bipy)₆](ClO₄)₄, **5.** A 0.109 g (0.696 mmol) sample of 2,2'-bipy was added to a yellow solution of **2** (0.200 g, 0.087 mmol) (molar ratio 8:1, Ag:bipy

1:1) in 30 mL of acetone, and the mixture was stirred for 6 h. The solvent was removed, and the residue was dissolved in CHCl₃ (10 mL) and then *n*-hexane was added (5 mL). On slow evaporation of this mixture, **5** is obtained as a microcrystalline yellow pale solid in 58% yield. Similar results were obtained by treating **2** with 6 equiv of bipy: 0.2 g of **2** (0.087 mmol) and 0.0815 g (0.522 mmol) of bipy (44% yield). Anal. Calcd for Ag₈C₁₀₈Cl₄H₁₂₄N₁₂O₁₆Pt₂: C, 40.07; H, 3.74; N, 5.19. Found: C, 40.00; H, 3.45; N, 5.68. MS FAB(+): *m/z* 3046 ([**1**)₂Ag]⁺, 4), 1579 ([**1**Ag]⁺, 100), 1227 ([Pt₂Ag₄(C≡C-*t*-Bu)₅]⁺, 34), peaks at *m/z* 1720 (50%), 1008 (35%), 898 (50%) and 790 (26%) are also observed. *es*(+): *m/z* 1785 ([Pt₂Ag₆(C≡C-*t*-Bu)₈(ClO₄)₂]⁺, 30), 1577 ([**1**Ag-2]⁺, 70), 1256 ([Pt₂Ag₂(C≡C-*t*-Bu)₈+1]⁺, 25), 421 ([Ag(bipy)₂+2]⁺, 100). Λ_M (in nitromethane solution): 472 Ω⁻¹ cm² mol⁻¹. IR (KBr, ν_{max} /cm⁻¹): 2047 (w), 2010 (m) (C≡C), 1092 (vs,br), 621 (vs) (ClO₄⁻ stretching and bending), 1590 (s), 1579 (s), 1559 (m), 763 (sh), 758 (vs), 734 (s) (bipy). ¹H NMR (CDCl₃): δ 8.80 (s, br), 8.33 (d, *J* = 7.9), 8.00 (st, *J* ~ 7.3), 7.49 (st, *J* ~ 5.3) (bipy), 1.23 (s, *t*-Bu).

X-ray Diffraction Study. Table 4 reports details of the structure analyses for complexes **3** and **4**. A green prismatic crystal of **3** was fixed with high-vacuum grease on top of a glass fiber, and a pale-green prismatic crystal of **4** was fixed with epoxy on top of a glass fiber. The diffraction measurements were made at room temperature for **3** on a NONIUS κ CCD and at 200 K for **4** on an automatic four-circle diffractometer Siemens P4, using graphite-monochromated Mo K α radiation. No crystal decay was observed over the data collection period. The structures were solved by direct methods and refined by using full-matrix least-squares refinement on *F*² with the SHELXL-97 program.²¹ All non-hydrogen atoms were located in succeeding difference Fourier syntheses and refined with anisotropic thermal parameters except for **4**; six C atoms (C10, C11, C12, C10', C11', and C12' that correspond

(21) Sheldrick, G. M. *SHELXL-93, program for crystal structure determination from diffraction data*; University of Göttingen: Germany, 1997.

to CH₃ groups disordered over two positions) and eight O atoms (O5 to O12) were refined at half-occupancy with isotropic displacement parameters. All hydrogen atoms were constrained to idealized geometries and assigned isotropic displacement parameters 1.2 times the U_{iso} value of their attached carbon for the aromatic hydrogens and 1.5 times that for the methyl hydrogens. Both molecules are centrosymmetric, and therefore only half of the molecule was used for the resolution of the crystal structure.

In **4**, H atoms were not added for atoms C10, C11, C12, C10', C11', and C12'. The ClO₄ groups occupy three sites. In one of them the ClO₄ was located in a general position and refined at full occupancy. In the two others the perchlorate was refined at half-occupancy; the Cl atom lies over a symmetry axis, and the O atoms are disordered over two positions in the full molecule. Final difference electron density maps showed no features outside the range 1.329 to $-1.825 \text{ e } \text{Å}^{-3}$ for **3** and 1.117 to $-0.699 \text{ e } \text{Å}^{-3}$ for **4**.

Computational Details. Extended Hückel calculations were carried out using the CACAO program.¹⁹ For [Pt(C≡C-*t*-Bu)₄]²⁻ a C_{4v} symmetry was used and D_4 for [Pt₂Ag₄(C≡C-

t-Bu)₈], with a staggered conformation, torsion angle 45° [C_α-Pt(1)-Pt(2)-C_α]. The following bond lengths were used: Pt-C_α 2.00 Å, C_α-C_β 1.20 Å, C_β-C_γ 1.40 Å, Pt(1)-Pt(2) 4.20 Å, Ag-Pt 3.15 Å, Ag-C_α 2.29 Å and Ag-C_β 2.51 Å.

Acknowledgment. Financial support was generously provided by the Dirección General de Investigación Científica y Técnica (Spain, Projects PB98-1595-C02-01,02) and the University of La Rioja (Project API-99/B17 and a grant for J.G.).

Supporting Information Available: Tables of full atomic positional and equivalent isotropic displacement parameters, anisotropic displacement parameters, full bond distances and bond angles, and hydrogen coordinates and isotropic displacement parameters for the crystal structures of complexes **3** and **4**. This material is available free of charge via the Internet at <http://pubs.acs.org>.

OM0001570